IEEE Access
Multidisciplinary ⋮ Rapid Review ⋮ Open Access Journal

Received 27 May 2025, accepted 7 July 2025, date of publication 16 July 2025, date of current version 30 July 2025.

Digital Object Identifier 10.1109/ACCESS.2025.3589390

RESEARCH ARTICLE

A Dual-Branch Deep Learning Framework Combining Xception and ResNet for Accurate Lung and Colon Cancer Detection

CHANDRASEKAR VENKATACHALAM[1] AND PRIYANKA SHAH[2]
[1]Department of CSE (AIML), Faculty of Engineering and Technology, JAIN (Deemed-to-be-University), Bangalore, Karnataka 562112, India
[2]Department of CSE, Faculty of Engineering and Technology, JAIN (Deemed-to-be-University), Bangalore, Karnataka 562112, India

Corresponding author: Chandrasekar Venkatachalam (Chandrasekar.v@jainuniversity.ac.in)

ABSTRACT Lung and colon cancers are among the leading causes of cancer-related deaths worldwide. Early detection significantly enhances survival rates, but traditional diagnostic methods, which rely on manual analysis of histopathological images, are labor-intensive, error-prone, and inconsistent. While deep learning has shown promise in automating medical image analysis, existing models often struggle with issues like overfitting, poor generalization, and class imbalance, which limit their clinical effectiveness. This research proposes a hybrid deep learning model combining the strengths of Xception and ResNet architectures. The Xception model excels at feature extraction, while ResNet's residual connections improve training stability and address issues like gradient vanishing. The model is trained using a large dataset of lung and colon cancer images, with a dynamic learning rate and backpropagation via Stochastic Gradient Descent (SGD) momentum, optimizing performance. Advanced data augmentation techniques, such as rotations and flips, further enhance model generalization. The proposed hybrid model achieves an impressive accuracy of 98.96%, demonstrating high effectiveness in distinguishing between different cancer classes. The model outperforms traditional diagnostic methods, offering a robust and reliable tool for automated cancer detection with significant clinical potential.

INDEX TERMS Lung cancer, colon cancer, histopathological images, Xception, ResNet, stochastic gradient descent, backpropagation.

I. INTRODUCTION

A. BASIC INTRODUCTION ABOUT THE PROBLEM WITH ALL DETAILS

Cancer continues to be one of the most pressing health challenges of our time, claiming millions of lives each year and placing an immense burden on individuals, families, and healthcare systems across the globe [1]. Among the wide range of cancers, lung and colon cancer stand out not only because of their high prevalence but also due to the severity of outcomes they often lead to. Lung cancer, largely driven by smoking and environmental toxins, remains the leading cause of cancer-related deaths worldwide [2]. A major concern is that it is frequently diagnosed at an advanced stage—when treatment options are limited and survival rates drop dramatically. Colon cancer, while more treatable if caught early, still ranks among the top causes of cancer deaths globally. In both cases, early and accurate diagnosis is critical to improving survival chances and quality of life. Traditionally, diagnosing these cancers relies heavily on techniques such as CT scans, X-rays, and endoscopic procedures. While these methods have been the gold standard for decades, they are not without limitations. Their accuracy depends largely on the skill and judgment of radiologists and pathologists, which can vary from one expert to another. Human fatigue, subtle differences in images, and the growing workload in hospitals can all contribute to misdiagnoses or delayed results—costing precious time in a disease where every moment matters [3].

This is where artificial intelligence (AI), and more specifically deep learning, is beginning to make a meaningful

The associate editor coordinating the review of this manuscript and approving it for publication was Olarik Surinta.

impact. Recent advances in AI have introduced tools that can support medical professionals by automating parts of the diagnostic process. Convolutional Neural Networks (CNNs)—a type of deep learning model—are particularly well-suited for analyzing medical images. These models can detect patterns and features that might not be immediately visible to the human eye, enabling more consistent and rapid interpretations of scans. The potential here is enormous: quicker diagnoses, fewer errors, and earlier interventions that can save lives [4].

However, harnessing this potential is not without challenges. Building effective AI models for healthcare requires not only a large volume of high-quality data but also models that can generalize well across different patient populations and imaging devices. Another important concern is interpretability—ensuring that the decisions made by AI are understandable and trustworthy for clinicians. Choosing the right deep learning architecture and fine-tuning it appropriately is also a critical part of the process [5].

In this research, we explore the use of two advanced deep learning architectures—Xception and ResNet—to develop a model capable of classifying lung and colon cancer images with high precision. By combining the strengths of both models, we aim to create a system that enhances the accuracy and reliability of cancer diagnosis. Our goal is to support clinicians by providing an intelligent tool that can assist in early detection, reduce diagnostic errors, and ultimately contribute to better patient outcomes through timely treatment.

B. MOTIVATION

The motivation for this research stems from the increasing need for automated systems that can support medical professionals in making accurate and timely diagnoses. The advent of deep learning techniques, particularly convolutional neural networks (CNNs), has shown great promise in medical image analysis, offering an opportunity to develop systems that can reliably assist in the early detection of lung and colon cancers. Despite the potential of these techniques, several challenges remain in terms of dataset diversity, model interpretability, and generalization to real-world clinical settings. The primary motivations for this study include:

Improving Early Detection: Early detection of lung and colon cancer significantly increases survival rates. By automating the process of analyzing medical images, deep learning models can aid in identifying cancerous lesions at early stages, improving the accuracy and speed of diagnosis.

Reducing Human Error: Human doctors and radiologists can make errors in diagnosis due to the overwhelming volume of medical images to analyze, variations in image quality, and fatigue. Deep learning models can serve as a supportive tool to reduce these errors and provide a more consistent evaluation of medical images.

Advancing Healthcare through AI: The integration of artificial intelligence (AI) and machine learning models in healthcare is a growing field. Our research aims to contribute to this field by developing reliable, efficient models that can assist in cancer detection and classification.

C. OBJECTIVE OF THE RESEARCH PAPER

The primary objective of our research paper is to develop and evaluate deep learning models that can automatically classify lung and colon cancer from medical image datasets. In this work, we focus on two state-of-the-art architectures: Xception and ResNet, both of which are known for their performance in image classification tasks. The contributions of this research are:

Model Development: We propose and implement deep learning models, specifically Xception and ResNet, for classifying lung and colon cancer types using a large dataset of labeled medical images. These models are designed to handle the complexities and variations in medical image data.

Data Preprocessing Pipeline: A comprehensive preprocessing pipeline is developed to clean, augment, and prepare the medical image data for training the models. This ensures the robustness of the models and improves their ability to generalize to unseen data.

Performance Evaluation: We thoroughly evaluate the models using various performance metrics, including accuracy, precision, recall, F1-score, and AUC. We also compare the performance of Xception and ResNet models, highlighting the strengths and weaknesses of each approach.

Model Optimization: The research includes an exploration of different hyperparameter optimization techniques and training strategies, focusing on improving model convergence, reducing overfitting, and achieving high accuracy on test data.

This paper aims to contribute to the growing body of work that leverages deep learning in medical image analysis and seeks to enhance early cancer detection using AI technologies.

II. LITERATURE SURVEY

The diagnosis of lung and colon cancer, particularly from histopathological images, has long been a challenging task due to the complexity and variability of tissue structures. With advances in computational techniques, automated methods have increasingly been employed to aid pathologists in diagnosing these cancers more accurately and efficiently. This literature survey explores the evolution of diagnostic methods, highlighting traditional and modern deep learning approaches, and identifies the challenges and opportunities in the field.

A. TRADITIONAL METHODS IN CANCER DIAGNOSIS

Traditional image analysis techniques relied heavily on manual feature extraction, where specific characteristics of the cancer cells, such as texture, shape, and color, were manually defined. These features were then fed into machine learning models like Support Vector Machines (SVM) and Random Forests for classification. However, these methods

often struggled with capturing complex patterns and had limitations when dealing with large, unstructured datasets [6].

B. DEEP LEARNING APPROACHES

Deep learning, particularly Convolutional Neural Networks (CNNs), has revolutionized the field of medical image analysis. These networks can automatically learn hierarchical feature representations from raw image data, making them well-suited for tasks like detecting tumors and classifying tissue types [7]. CNNs have been successfully applied to lung and colon cancer detection, demonstrating the ability to learn complex patterns from histopathological images without manual intervention.

C. HYBRID AND ADVANCED ARCHITECTURES

Hybrid models that combine multiple deep learning architectures, such as ResNet and Xception, have been developed to enhance performance. ResNet, with its residual connections, mitigates the vanishing gradient problem, while Xception, with its depthwise separable convolutions, reduces computational costs [8]. These architectures capture both low- and high-level image features, improving diagnostic accuracy. The integration of such models allows for the automatic learning of complex features from histopathological images.

D. TRANSFER LEARNING AND PRETRAINED MODELS

Transfer learning, the practice of leveraging pretrained models (such as those trained on ImageNet) and fine-tuning them for medical image tasks, has become a standard approach. This allows for high model accuracy despite limited labeled datasets, which are often a challenge in the medical field. Fine-tuning networks like ResNet and Xception on specialized medical datasets facilitates the learning of useful feature representations and enhances model performance.

E. DATA AUGMENTATION AND HANDLING CLASS IMBALANCE

Data augmentation techniques, including rotation, flipping, scaling, and brightness adjustments, are used to artificially expand the training dataset, helping to improve model generalization and reduce overfitting. Class imbalance, where some cancer types are underrepresented, is a common issue. Solutions like oversampling minority classes, under sampling majority classes, or employing focal loss functions are used to ensure models are not biased toward the majority class [9].

F. EVALUATION METRICS IN CANCER DIAGNOSIS

The evaluation of model performance involves various metrics. Accuracy, while common, often does not fully capture model performance, particularly in cases of class imbalance. Precision, recall, and the F1-score offer a more nuanced view of the model's ability. The Area Under the Curve (AUC) is another critical metric, especially for imbalanced datasets. These metrics are essential for assessing the practical utility of models in clinical settings, where the cost of misdiagnosis can be significant [10].

G. CHALLENGES AND FUTURE DIRECTIONS

Despite advancements, challenges persist, including the need for large, high-quality labeled datasets, the interpretability of deep learning models, and handling class imbalance. Future directions include developing techniques for model explainability, integrating multimodal data (clinical information alongside histopathological images), and improving generalization across cancer subtypes. Research will focus on advancing model performance through hybrid architectures and ensuring practical integration of these models into real-world clinical workflows. Table 1 represents the related work.

Despite the significant advancements in cancer diagnosis using deep learning, several challenges persist that hinder the full potential of automated diagnostic systems. One of the main gaps is the need for large, high-quality labeled datasets, which are often unavailable in the medical domain due to privacy concerns, high costs, and time constraints. Furthermore, traditional methods struggle with handling class imbalances and the complex, varied nature of cancerous tissues across different patients. Although transfer learning has been a powerful solution to this problem, models still struggle with generalization across diverse datasets and may not always perform well on unseen data. Additionally, the interpretability of deep learning models in clinical settings remains a challenge, limiting their acceptance by healthcare professionals who require explainable decisions to trust AI systems for diagnosis.

Our approach aims to address these gaps by leveraging a hybrid deep learning model combining state-of-the-art architecture like ResNet and Xception, with transfer learning techniques to overcome the limitations of small datasets. Through extensive data augmentation and careful handling of class imbalance, our model is optimized for both accuracy and generalization across various subtypes of lung and colon cancer. Additionally, our methodology focuses on model explainability, ensuring that the results produced by the system can be understood and trusted by clinicians. By combining these strategies, our approach offers a robust solution for accurate, efficient, and interpretable cancer diagnosis from histopathological images, thus bridging the gaps present in existing methodologies.

III. PROPOSED METHODOLOGY

A. ARCHITECTURE DIAGRAM

The proposed hybrid deep learning model integrates two state-of-the-art convolutional neural network (CNN) architectures—Xception and ResNet—to enhance classification accuracy in lung and colon cancer image analysis. The model leverages the strengths of both networks through a structured pipeline, consisting of the following components:

TABLE 1. Related work from the existing research.

Research	Objective	Summary
Sobur, Abdus, et al., (2024) [11]	To design a hybrid deep learning model for efficient classification of lung and colon cancer from histopathological images.	The model provides a robust and reliable solution for cancer classification, advancing medical image analysis techniques.
Seth, Amit, et al. (2024) [12]	To develop a deep learning-based method integrating preprocessing, segmentation, and classification phases for efficient lung and colon cancer diagnosis from histopathological images.	The proposed methodology streamlines cancer detection, offering an effective solution for diagnosing lung and colon cancers through advanced segmentation and classification techniques.
Borah, Nayana, et al., (2024) [13]	To develop a modified deep learning framework for early detection of lung and colon cancers by integrating feature reduction and adaptive diagnostic techniques.	The framework enhances data representation and diagnostic efficiency, offering a superior solution for complex cancer detection scenarios.
Suominen, Mirka, et al., (2024) [14]	To explore deep learning and feature extraction techniques for classifying histopathological images of colon cancer, aiming to enhance diagnostic accuracy and efficiency.	Deep learning proves to be an effective tool in colon cancer diagnosis, supporting pathologists in reducing delays and improving prognostic outcomes.
Gago-Fabero, Álvaro, et al. (2024) [8]	To develop and optimize low-computational CNN architectures for binary classification of colorectal cancer from histopathological images, ensuring high accuracy and reduced computational costs.	The optimized architecture demonstrates robust performance, offering an efficient and accurate solution for colorectal cancer screening with significantly reduced computational demands.
Al-Mamun Provath, Md, Kaushik Deb, et al. (2023) [15]	To develop a computationally efficient and accurate CNN-based model for early detection of lung and colon cancer using the LC25000 dataset.	The proposed model effectively addresses inter-class variations and provides a robust solution for precise cancer detection, surpassing existing methods in efficiency and performance.
Khan, Ammar Ahmad, et al. (2023) [16]	To develop and evaluate a deep learning model utilizing Vision Transformers and Swin Transformer for accurate classification of colon cancer from histopathological images.	The proposed modified Swin Transformer demonstrates superior performance, providing a robust solution for colon cancer identification and classification.
Tummala, Sudhakar, et al. (2023) [17]	To develop an automated method using EfficientNetV2 models for subtype classification of lung and colon cancers from histopathological images, ensuring accuracy and explainability.	The proposed pipeline demonstrates state-of-the-art performance and provides visual explainability, making it a promising tool for clinical cancer diagnosis and treatment planning.
Stephen, Okeke, et al. (2023) [18]	To develop an efficient neural network architecture for lung and colon cancer	The proposed model achieves landmark performance in cancer

TABLE 1. *(Continued.)* **Related work from the existing research.**

	detection using a Bayesian convolutional neural architectural search algorithm combined with Gaussian processes.	classification, optimizing architecture selection and improving both training efficiency and accuracy.
Luo, Ruihao, et al. (2023) [19]	To investigate transfer learning techniques for binary classification of colorectal cancer, focusing on fine	The study demonstrates that adding convolutional layers enhances model performance, providing a valuable strategy for transfer learning in biomedical image analysis.
Deiva Nayagam, et al. (2025) [31]	To develop an accurate and efficient deep learning model using ResNet101 with transfer learning for classifying colorectal cancer as benign or malignant from histopathological images.	The proposed model effectively enhances the accuracy and reliability of colorectal cancer classification, demonstrating its potential over traditional CNN approaches.
Pasha, MD Azam, et al. (2025) [32]	To develop an optimized deep learning framework integrating VGG16, ResNet, and SC-JAO for early and accurate detection of lung and colon cancer from histopathological images.	The proposed model effectively enhances cancer detection performance by leveraging multi-level feature extraction and optimization, demonstrating superiority over conventional methods.

1) INPUT LAYER

The model accepts histopathological images from the LC25000 dataset, representing various lung and colon cancer types. All images are resized to 512 × 512 pixels to maintain uniformity. Preprocessing steps such as normalization (scaling pixel values between 0 and 1) and data augmentation (including rotation, flipping, and zoom) are applied to improve the robustness and generalization capability of the model.

2) PRE-TRAINED FEATURE EXTACTION

Xception Branch: Xception employs depthwise separable convolutions, which effectively reduce computational cost while capturing fine-grained spatial features. It is particularly suitable for medical image analysis due to its strong localization ability.

ResNet Branch: ResNet utilizes residual connections that enable deeper network training by preventing gradient vanishing. This ensures better feature learning and helps in extracting both low-level and high-level image patterns.

Both networks are initialized with ImageNet pre-trained weights and fine-tuned using the cancer image dataset to adapt to domain-specific characteristics.

3) FEATURE FUSION LAYER

The feature maps obtained from the Xception and ResNet models are concatenated into a unified representation. This fused vector combines diverse visual features, enhancing the model's ability to distinguish between subtle morphological differences in cancer tissues.

A Global Average Pooling (GAP) layer follows the fusion, reducing the dimensionality of the combined feature map into a single compact feature vector per image. This reduces overfitting while preserving relevant information.

4) FULLY CONNECTED LAYER

The feature vector is passed through a series of dense layers equipped with ReLU activation functions. Dropout layers are also included for regularization to minimize overfitting. The final dense layer uses a Softmax activation function to generate probabilities across five output classes: Lung Adenocarcinoma, Lung Squamous Cell Carcinoma, Colon Adenocarcinoma, Normal Lung Tissue, Normal Colon Tissue.

5) OUTPUT LAYER

The class with the highest probability score is selected as the model's final prediction. Along with the prediction, the model logs confidence levels, error margins, and misclassified instances for detailed performance evaluation.

As illustrated in Figure 1, our proposed hybrid framework comprises two parallel deep learning branches: Xception and ResNet. These operate independently to extract spatial and semantic features, respectively. Their outputs are passed

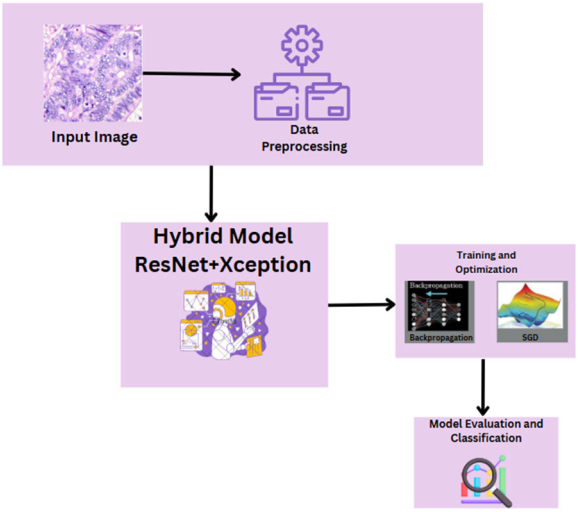

FIGURE 1. Architecture diagram of proposed model.

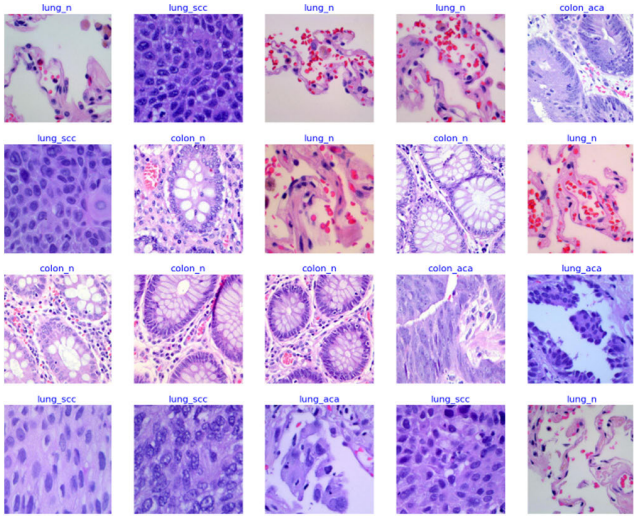

FIGURE 2. Sample images from the dataset.

through a late-fusion layer and an adaptive decision module that learns to weigh and combine features dynamically. This approach promotes deeper feature interaction and improves classification performance beyond simple concatenation.

B. DATA PREPROCESSING

In our lung and colon cancer classification project, we implemented several data preprocessing steps to prepare the dataset for model training and ensure that the neural network could effectively learn the patterns in the image data. The preprocessing pipeline was built around optimizing data augmentation, normalization, and efficient data handling. Below is a detailed explanation of the preprocessing steps followed in the project.

1) DATASET ORGANIZATION

The LC25000 dataset, used in this study, is a comprehensive collection of 25,000 histopathological images designed for lung and colon cancer classification. Each image is in JPEG format with a resolution of 768 × 768 pixels, ensuring high-quality input for deep learning models. Derived from HIPAA-compliant sources, the dataset initially consisted of 750 images of lung tissue (250 benign, 250 adenocarcinomas, and 250 squamous cell carcinomas) and 500 images of colon tissue (250 benign and 250 adenocarcinomas). Using the Augmenter package, data augmentation techniques such as rotation, scaling, flipping, and bright adjustments were applied to expand the dataset to 25,000 images, with each of the five classes (lung benign tissue, lung adenocarcinoma, lung squamous cell carcinoma, colon adenocarcinoma, and colon benign tissue) containing 5,000 images. Fig 2 depicts the sample images from the dataset.

While whole-slide image (WSI) datasets such as ACD-CLungHP and TCGA-LUAD offer detailed, large-scale histopathological views that reflect real-world clinical challenges, they often require specialized infrastructure, significant computational resources, and expert-level pixel-wise annotations. In contrast, the LC25000 dataset provides a curated, patch-level collection of histopathology images that are readily available, well-labeled, and balanced across classes, making it a practical choice for initial experimentation and benchmarking of deep learning models. Given its simplicity, clarity, and continued relevance in many recent publications, LC25000 remains a valuable dataset, particularly in research environments where access to WSIs is limited or not feasible. Therefore, it was selected for this study to validate the effectiveness of our dual-architecture model and to establish a strong foundation before transitioning to more complex datasets.

2) DATA AUGMENTATION

Data augmentation was performed to artificially expand the dataset, helping the model generalize better and prevent overfitting. We applied several transformations on the images, which included:

Rotation: Random rotations were applied to the images. The rotation angle θ was chosen randomly within a predefined range, e.g., between -30° and 30°. The transformation can be mathematically represented in equation 1.

$$x' = \boldsymbol{\alpha}.\boldsymbol{x} \tag{1}$$

where $\boldsymbol{R_\theta}$ is the rotation matrix, and θ is the randomly selected angle.

Translation (Shifting): We performed random shifts along the x-axis and y-axis. This transformation was applied using equation 2.

$$x' = x + \Delta x, y' = y + \Delta y \tag{2}$$

where Δx and Δy are random values drawn from a uniform distribution to shift the image horizontally and vertically.

Zooming: The zoom factor α was randomly selected within a range of 0.8 to 1.2, representing a zoom-in or zoom-out effect.

Flipping: Horizontal flipping was performed randomly with a probability of 50%, which was achieved by reversing the image along its vertical axis using equation 3.

$$x' = F(x) \tag{3}$$

where F(x) represents the flipping operation.

Brightness Adjustment: The brightness of each image was adjusted by a random factor β, chosen from the range [0.8, 1.2]. The brightness adjustment formula is given in equation 4.

$$\mathrm{x}' = \mathrm{x} \cdot \beta \tag{4}$$

By applying these transformations in a randomized manner, we ensured that the model learned to recognize features invariant to these changes, thereby improving its robustness.

Image Normalization: To normalize the pixel values of the images, we scaled the pixel values to a range of 0 to 1 by dividing each pixel by 255, as the original pixel values range from 0 to 255. This normalization formula is given in equation 5.

$$\boldsymbol{x_{norm}} = \frac{\boldsymbol{x}}{\mathbf{255}} \tag{5}$$

where x is the original pixel value and $\boldsymbol{x_{norm}}$ is the normalized pixel value in the range [0, 1].

This normalization step helps in speeding up the convergence of the model by ensuring that all input features (pixels) have the same scale. It also helps in preventing any one feature from dominating the others during the training process.

In addition, we used Z-score normalization in some cases, particularly when preprocessing images for training the models. This method ensures that the data has a mean of 0 and a standard deviation of 1, helping with faster convergence. This is represent in equation 6.

$$\boldsymbol{x_{norm}} = \frac{\boldsymbol{x} - \boldsymbol{\mu}}{\boldsymbol{\sigma}} \tag{6}$$

where μ is the mean pixel value across the dataset and σ is the standard deviation of the pixel values across the dataset.

Label Encoding: Since the dataset contains categorical labels representing the cancer types, we performed One-Hot Encoding to convert these categorical labels into numerical vectors. Each class label is represented as a binary vector where only the index corresponding to the class is set to 1, and all other positions are set to 0.

Data Splitting: The data was divided into training, validation, and test sets using the following proportions:

- Training Set: 70% of the total dataset.
- Validation Set: 15% for hyperparameter tuning and model evaluation during training.
- Test Set: 15% used exclusively for evaluating the final model.

This division ensures that the model is trained on a large portion of the data, validated on a separate set, and tested on an entirely unseen set to simulate real-world performance.

Class Balancing: Given the class imbalance observed in the dataset, where some cancer types were overrepresented while others were underrepresented, we implemented class balancing to ensure the model performed well across all classes. We did this by adjusting the loss function to assign higher weights to underrepresented classes.

The weighted loss function $L_{weighted}$ was computed using equation 7.

$$L_{\boldsymbol{weighted}} = \sum_{\boldsymbol{i}=1}^{N} \omega_{y_i} \cdot \boldsymbol{\mathcal{L}}\left(y_i, \widehat{y_i}\right) \tag{7}$$

where w_{yi} is the weight assigned to class yi inversely proportional to the class frequency, $\boldsymbol{L(y_i, \hat{y}_i)}$ is the loss for sample i, where $\boldsymbol{y_i}$ is the true label and $\hat{y}_i$ is the predicted label and N is the total number of samples in the batch. This technique ensured that the model paid more attention to the underrepresented classes, such as lung_scc, which had fewer samples compared to others. Batch Preparation: To optimize training, we utilized mini-batch gradient descent, which allowed us to train the model using batches of images rather than the entire dataset at once. The batch size was set to 32, and the loss was calculated as the average over each batch. For each batch, the gradient update rule is represent in equation 8.

$$\theta_{\boldsymbol{new}} = \theta_{\boldsymbol{old}} - \frac{\eta}{\beta} \sum_{i=1}^{B} \nabla_{\theta} \boldsymbol{\mathcal{L}}\left(x_i, y_i\right) \tag{8}$$

where Θ represents the model's parameters (weights and biases), η is the learning rate., B is the batch size, $\boldsymbol{x_i}$ and $\boldsymbol{y_i}$ are the features and labels of the i-th sample in the batch. The mini-batch approach helped in reducing memory consumption while providing efficient updates to the model's parameters.

C. DEEP LEARNING TECHNIQUES

In our lung and colon cancer classification project, the main objective was to build a deep learning model that could accurately classify medical images into cancerous and non-cancerous categories. To achieve this goal, we leveraged deep learning techniques, with a particular focus on using Xception and ResNet models. These models were chosen due to their exceptional performance in image classification tasks and their ability to handle the complex patterns found in medical images. Below, we explore the rationale behind the selection of these models, the training strategies, optimization methods, and the advantages these techniques offer in building high-performance models for cancer classification.

1) CONVOLUTIONAL NEURAL NETWORKS (CNN): THE BACKBONE OF IMAGE CLASSIFICATION

The backbone of our approach to cancer classification is based on Convolutional Neural Networks (CNNs). CNNs are a type of deep neural network that is particularly suited for image-based tasks. Unlike traditional machine learning algorithms, which require manual feature extraction, CNNs are

capable of automatic feature extraction by learning relevant features from raw input images. This allows CNNs to identify complex patterns in medical images without needing expert intervention for feature engineering.

2) SIGNIFICANCE OF USING CNN FOR CANCER CLASSIFICATION

Convolutional Neural Networks (CNNs) have revolutionized medical image analysis due to their ability to automatically learn hierarchical features directly from raw images. Unlike traditional machine learning methods that rely on handcrafted features, CNNs extract spatial patterns such as edges, textures, and shapes critical for identifying abnormalities in histopathological and radiological images. This capability makes CNNs particularly suited for cancer classification tasks, where subtle morphological differences between malignant and benign tissues must be discerned accurately. Furthermore, CNNs exhibit robustness to image noise and variations in staining or imaging conditions, which are common challenges in clinical datasets. Their proven success in numerous cancer detection studies highlights CNNs as a powerful tool for developing reliable and scalable diagnostic models, motivating their use in this work. Mathematically, the process of convolution in CNNs can be seen in equation 9.

$$y(t) = (x * \boldsymbol{\omega})(t) = \sum_{\tau} \boldsymbol{x}(\boldsymbol{\tau})\boldsymbol{\omega}(\boldsymbol{t} - \boldsymbol{\tau}) \tag{9}$$

Where x represents the input image, w represents the convolutional filter (kernel) and y(t) is the feature map generated by applying the filter to the image. By applying convolution operations repeatedly, CNNs build progressively higher-level features, leading to improved classification performance.

3) MODEL SELECTION: XCEPTION & RESNET

To develop a highly accurate system for cancer classification, we carefully selected two powerful deep learning architectures—Xception and ResNet. Both are advanced forms of convolutional neural networks (CNNs) that address key challenges in training deep models, such as overfitting, vanishing gradients, and high computational demands. Our choice was based on their proven ability to capture complex patterns in image data while maintaining efficiency and robustness. Xception (Extreme Inception): Xception is a highly advanced deep learning architecture that builds upon the Inception model by replacing traditional convolutions with depthwise separable convolutions. This modification significantly reduces the number of parameters in the model, making it more computationally efficient while maintaining high classification accuracy. Depthwise Separable Convolutions: Xception's key feature is the depthwise separable convolution, where the convolution operation is split into two smaller operations—depthwise convolution (which applies a single filter to each input channel) and pointwise convolution (which combines the outputs of the depthwise convolutions using 1×1 convolutions). This reduces the number of parameters and computation, making the model faster and more memory efficient. The depthwise separable convolution operation is represented in equation 10.

$$Y = \left(W_{\text{depthwise}} * X\right) * W_{\text{pointwise}} \tag{10}$$

$\boldsymbol{W_{depthwise}}$ is the set of depthwise convolution filters applied to each channel of the input image and $\boldsymbol{W_{pointwise}}$ is the 1×1 convolution filter that combines the outputs of the depthwise convolutions. ResNet (Residual Networks): ResNet introduced a groundbreaking concept in deep learning: residual connections. These connections allow the network to skip certain layers and pass information directly to deeper layers. This helps to mitigate the issue of vanishing gradients and allows the model to train deeper networks more effectively. Residual Learning: In a traditional neural network, deeper models face the problem of vanishing gradients, where gradients become too small to effectively update weights during backpropagation. ResNet solves this problem by introducing skip connections, allowing gradients to flow directly through the residual connections. The mathematical expression for a residual block is represented in equation 11.

$$Y = F(x, \{\boldsymbol{W_i}\}) + x \tag{11}$$

Where $F(x, \{\mathbf{W_i}\})$ represents the learned residual function, which is the output of the block after the layers, and x is the input to the block, which is directly added to the output of the residual function. The proposed hybrid model architecture consists of a dual-branch feature extraction design where Xception and ResNet models are individually fine-tuned and optimized. A novel aspect of this architecture lies in the late-fusion mechanism: feature vectors extracted from both branches are concatenated and passed through a fully connected decision layer trained from scratch. Unlike traditional ensemble methods, our approach integrates both spatial and semantic features at the representational level, ensuring richer and more discriminative learning. We further introduced a dynamic fine-tuning strategy using selective layer freezing and unfreezing schedules across training epochs to optimize convergence and reduce overfitting.

4) TRAINING STRATEGY: BACKPROPAGATION, STOCHASTIC GRADIENT DESCENT(SGD) AND MOMENTUM

Training deep neural networks like Xception and ResNet requires sophisticated optimization techniques. Backpropagation is the core algorithm used for training neural networks. During backpropagation, the gradients of the loss function are computed with respect to the model's parameters, and these gradients are used to update the parameters via optimization techniques like Stochastic Gradient Descent (SGD). Backpropagation: In this process, the model iteratively updates its weights to minimize the loss function. The loss function quantifies the difference between predicted and true values, and the gradient of the loss is computed with respect to the weights of the model. This gradient is used to update the weights via an optimization method. Stochastic Gradient Descent (SGD): We use SGD as the primary optimization algorithm. Unlike batch gradient descent, which uses the

entire dataset for every weight update, SGD updates the weights using a randomly chosen mini-batch of the dataset, which speeds up the training process. The update rule for SGD with momentum is represent in equation 12.

$$v_t = \beta v_{t-1} + (1-\beta)\nabla_\theta J(\theta) \tag{12}$$

where $\boldsymbol{v_t}$ is the velocity (or accumulated gradient), β is the momentum coefficient, η is the learning rate, and J(θ) is the loss function. Momentum helps accelerate the gradient descent process by considering the previous weight updates, which makes it easier for the model to converge and helps it escape local minimum.

5) OPTIMIZATION METHODS: ADAM OPTIMIZER AND LEARNING RATE SCHEDULING

In addition to SGD, we incorporated the Adam optimizer and learning rate scheduling for further optimization and fine-tuning of our models. Adam Optimizer: The Adam optimizer combines the benefits of both AdaGrad and RMSprop, adapting the learning rate for each parameter based on first and second moment estimates of the gradients. The rule for Adam is represented in equation 13.

$$\hat{m}_t = \frac{\boldsymbol{m_t}}{\mathbf{1}-\boldsymbol{\beta_1^t}}, \hat{v}_t = \frac{\boldsymbol{v_t}}{\mathbf{1}-\boldsymbol{\beta_1^t}} \tag{13}$$

where $\boldsymbol{m_t}$ and $\boldsymbol{v_t}$ are the first and second moment estimates, respectively, and $\beta 1$ and $\beta 2$ are hyperparameters controlling the decay rates of the moving averages. Learning Rate Scheduling: Learning rate scheduling allows us to adjust the learning rate during training to improve convergence. We used step decay, which reduces the learning rate at certain intervals, ensuring that the model makes finer adjustments as it approaches the optimal solution. The learning rate scheduling formula is represented in equation 14.

$$\boldsymbol{\eta_t} = \boldsymbol{\eta_0}.\boldsymbol{decay\_rate}^{\frac{1}{\boldsymbol{decay\_steps}}} \tag{14}$$

where $\boldsymbol{\eta_t}$ is the learning rate at time step t, $\boldsymbol{\eta_0}$ is the initial learning rate and decay_rate controls how quickly the learning rate decreases.

6) STATISTICAL ANALYSIS

The statistical analysis of the proposed model was conducted to evaluate its classification performance in detecting and distinguishing lung and colon cancer subtypes. The following sections detail the metrics, visualizations, and methodologies used to assess the model's effectiveness.

7) CONFUSION MATRIX

The confusion matrix was used to summarize the classification model's performance by comparing predicted labels with actual labels. Each entry in the confusion matrix represents the count of predictions for a given true class and predicted class. Diagonal elements indicate correctly classified instances, while off-diagonal elements highlight misclassifications. This matrix is pivotal for identifying class-specific errors.

8) CLASSIFICATION REPORT METRICS

Performance metrics such as precision, recall, F1-score, and accuracy were computed to quantify the model's performance. Precision (P): Fraction of relevant instances among the retrieved instances which is represented as equation 15.

$$\text{Precision} = \frac{\text{TP}}{\text{TP+FP}} \tag{15}$$

Recall (R): Fraction of relevant instances that were correctly identified which is represented as equation 16.

$$\text{Recall} = \frac{\text{TP}}{\text{TP+FN}} \tag{16}$$

F1-Score: Harmonic mean of precision and recall which is represented as equation 17.

$$\boldsymbol{F1} = 2 \cdot \frac{\text{Precision} \times \text{Recall}}{\text{Precision+Recall}} \tag{17}$$

Accuracy: Overall proportion of correctly classified samples which is represented as equation 18.

$$Accuracy = \frac{\boldsymbol{Correct\ Predictions}}{\boldsymbol{Total\ Predictions}} \tag{18}$$

The classification report included these metrics for each class, as well as macro-averaged and weighted-average scores to provide a holistic view of model performance across imbalanced classes.

9) TRAINING AND VALIDATION METRICS

The model's training and validation performance were evaluated using loss and accuracy which is represented in equation 19.

$$\boldsymbol{Loss} = -\frac{\mathbf{1}}{\boldsymbol{N}} \sum_{\mathbf{i=1}}^{\boldsymbol{N}} \boldsymbol{y_i log(p_i)} \tag{19}$$

where N is total number of samples, $\boldsymbol{y_i}$ is True label for the i-th sample and $\boldsymbol{p_i}$ is Predicted probability of the true class for the i-th sample

Training and validation losses and accuracies were plotted to visualize the convergence and potential overfitting/underfitting during the model's learning process.

10) ERRORS BY CLASS ON TEST SET

Class-wise error distribution was analyzed to identify challenging classes where the model struggled. Errors for each class were calculates using equation 20.

$$\text{Errors per Class} = \sum_{k=1}^{N} \mathbf{1}(\boldsymbol{y_k} = \boldsymbol{c} \bigwedge \hat{y_k} \neq \boldsymbol{c}) \tag{20}$$

where c is the class being evaluated.

Bar plots were generated to visualize the number of errors per class, providing insights into the complexity and confusion between specific cancer subtypes.

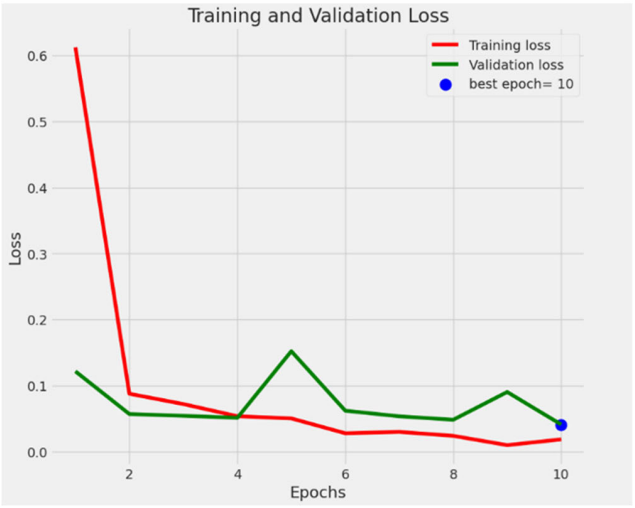

FIGURE 3. Training and validation loss.

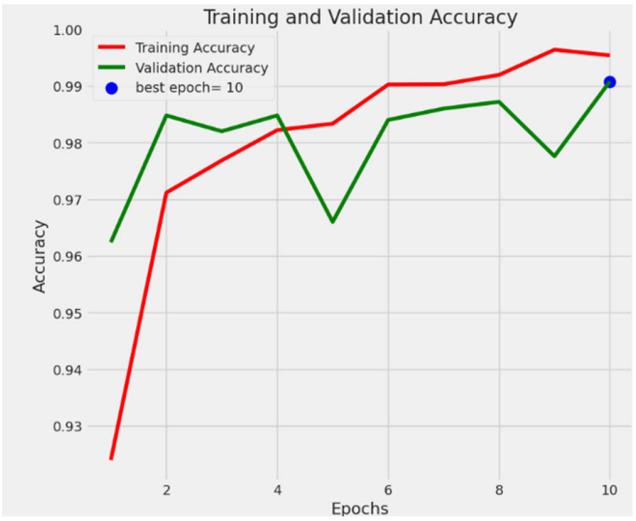

FIGURE 4. Training and validation accuracy.

IV. EXPERIMENT ANALYSIS AND RESULTS

This section presents a comprehensive analysis of the experimental results achieved during the classification of lung and colon cancer subtypes. It highlights the performance of the model in terms of training and validation metrics, test set evaluation, confusion matrix analysis, error distribution, threshold-independent metrics (Precision-Recall and ROC curves), and computational efficiency. The results provide a detailed understanding of the model's capabilities, limitations, and its potential for clinical applications.

A. TRAINING AND VALIDATION PERFORMANCE

The model training utilized a dataset of lung and colon cancer subtypes, employing categorical cross-entropy loss and Adam optimizer. The training process spanned multiple epochs, with training and validation performance metrics recorded for accuracy and loss. Fig 3 and Fig 4 depict the training and validation Loss and accuracy.

- The training accuracy peaked at 99.78%, demonstrating the model's ability to effectively learn complex features.
- The validation accuracy reached 99.21%, with the validation loss remaining closely aligned with the training loss, suggesting minimal overfitting and excellent generalization.
- These results reflect a well-optimized training process, with consistent performance across training and validation datasets.

B. TEST SET EVALUATION

The proposed model was evaluated on a held-out test set comprising 2,500 histopathological images, covering five cancer subtypes. The model achieved an overall accuracy of 98.96%, indicating robust generalization and reliable classification performance.

As summarized in Table 2, each class achieved precision and recall values above 96.00%, demonstrating the model's ability to accurately distinguish between cancer subtypes and minimize false positives and false negatives. The F1-scores ranged from 0.97 to 1.00, confirming balanced predictive performance across all classes.

These results highlight the model's high fidelity in identifying both lung and colon cancer categories with consistency.

C. CONFUSION MATRIX ANALYSIS

A confusion matrix was constructed to assess the model's predictions:

- The diagonal elements of the confusion matrix represented high true positive rates across all classes, indicating accurate classification.
- The off-diagonal elements were minimal, highlighting a low rate of misclassifications, which were primarily observed in classes with overlapping morphological features.

The confusion matrix provided a visual confirmation of the model's overall effectiveness, pinpointing areas for further enhancement. Fig 5 depicts the confusion matrix generated from our proposed model.

D. ERROR ANALYSIS

A detailed error analysis was conducted to understand the nature and distribution of misclassifications which is depict by Fig 6.

- A bar chart depicting errors by class revealed that the majority of errors occurred in specific subtypes, particularly where inter-class similarities were higher.
- Misclassified examples were analyzed, providing insights into possible feature extraction limitations.
- This analysis serves as a foundation for future improvements, such as incorporating advanced augmentation strategies or refining the model architecture.

TABLE 2. Classification report.

	Precision	Recall	F1-Score	Support
colon_aca	1.00	1.00	1.00	479
colon_n	1.00	1.00	1.00	518
lung_aca	0.99	0.96	0.97	488
lung_n	1.00	1.00	1.00	516
lung_scc	0.96	0.99	0.97	498
accuracy			0.99	2500
macro avg	0.99	0.99	0.99	2500
weighted avg	0.99	0.99	0.99	2500

1) COMPUTIONAL PERFORMANCE

The computational efficiency of the model was evaluated to determine its suitability for real-world applications:

Training Time: The model required 13,10.44 seconds to complete training, demonstrating an efficient optimization process for the given dataset size and complexity.

Inference Time: The model classified 2,500 test images in 87.66 seconds, equating to approximately 35.06 milliseconds per image.

Model Size: The final model size of 734.28 MB ensures deployability without compromising performance.

2) PERFORMANCE ACROSS CLASSES

Class-wise performance metrics provide deeper insights into the model's behavior:

- For colon adenocarcinoma (colon_aca) and colon normal (colon_n), both precision and recall were 100%, indicating perfect classification.

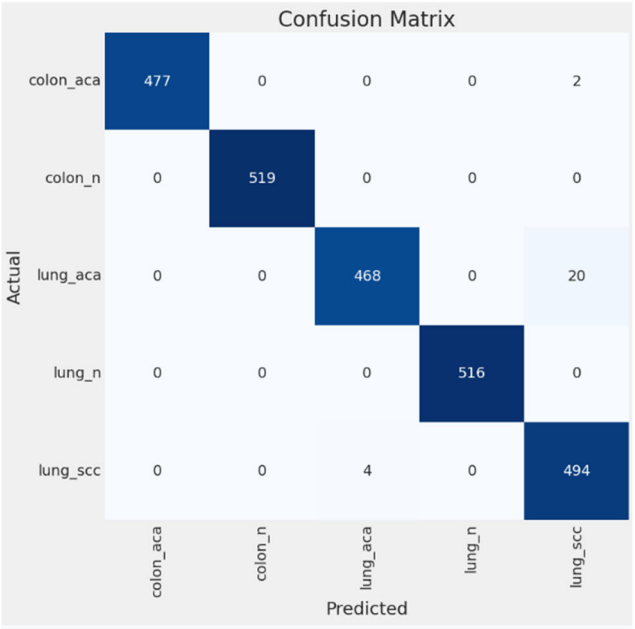

FIGURE 5. Confusion matrix.

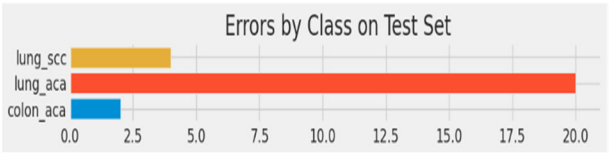

FIGURE 6. Errors by class on test set.

- For lung adenocarcinoma (lung_aca), a slight reduction in recall to 96.00% was observed, suggesting room for improvement in this class.
- Lung squamous cell carcinoma (lung_scc) showed a precision of 96.00% and recall of 99.00%, highlighting minor challenges in distinguishing it from other classes.

These metrics validate the model's ability to perform consistently across diverse cancer subtypes, with minimal performance variation.

The experimental findings highlight the effectiveness of the model for classifying lung and colon cancer subtypes. Key results include:

High Classification Accuracy: The model achieved an overall test accuracy of 98.96%.

Balanced Performance: Precision, recall, and F1-scores across all classes were consistently high, confirming the model's balanced classification ability.

Threshold-Independent Metrics: Near-perfect AUC-ROC and AUC-PR values affirm the model's robustness.

Low Misclassification Rates: Minimal errors were observed, primarily in classes with overlapping features.

Efficiency: The model demonstrated competitive computational performance, making it viable for clinical application.

These results position the model as a promising tool for aiding clinical diagnosis of lung and colon cancer

subtypes, offering high accuracy, reliability, and computational efficiency.

V. DISCUSSION

A. LIMITATIONS AND CHALLENGES

While deep learning models, particularly Xception and ResNet, show immense potential in the diagnosis of lung and colon cancers, their application comes with certain limitations and challenges that need to be addressed for real-world deployment.

- Dataset Size and Diversity: Large, diverse datasets are essential for generalization. Our model is trained on a relatively limited dataset, which may not cover all demographic and imaging variations, potentially affecting performance on unseen data.
- Data Imbalance: Medical datasets often have uneven class distributions, which can bias the model toward majority classes and reduce accuracy on rare cases.
- Dataset Limitation – LC25000: The LC25000 dataset, used in this study, consists of small histopathology image patches and lacks the complexity of whole-slide images (WSI) like ACDCLungHP or TCGA-LUAD. Although WSIs offer more clinically relevant information, they require significant resources and specialized annotation. LC25000 was chosen for its accessibility and use as a baseline; however, we plan to validate our approach on WSI datasets in future work.
- Interpretability: Deep learning models are often ''opaque systems,'' making it difficult to explain predictions, which can limit clinical trust and adoption.
- Ethical Considerations: AI use in healthcare raises privacy, security, and regulatory concerns that must be carefully managed.

While real-time clinical datasets offer invaluable opportunities for model validation and deployment, accessing such data is currently constrained by patient privacy laws, ethical approvals, and institutional protocols. Moreover, publicly available real-time datasets often lack the necessary size, diversity, and high-quality annotations required for effective training and evaluation. Therefore, this study employs the LC25000 dataset, which, despite being a patch-based dataset, remains a widely recognized benchmark in lung and colon cancer image classification research, facilitating direct comparison with prior works.

Our model is developed with adaptability in mind, allowing for seamless future application and validation on larger and more complex real-time datasets such as whole-slide images (WSIs) and clinical data, once such datasets become accessible. Future work will focus on acquiring and testing with these datasets to further assess the model's clinical utility and robustness.

B. ADVANTAGES OF PROPOSED MODEL

Despite the challenges mentioned above, the deep learning models proposed in this study—Xception and ResNet—offer several significant advantages, which make them particularly well-suited for cancer detection:

High Accuracy and Robustness: The combination of Xception and ResNet architecture allows the model to achieve high accuracy in classifying medical images. Xception's depthwise separable convolutions and ResNet's residual connections help in learning complex features from medical images while mitigating overfitting, ensuring robust performance across diverse test cases.

Ability to Detect Subtle Patterns: Deep learning models, especially CNNs, excel at detecting patterns in images that might not be easily visible to the human eye. This is crucial in early-stage cancer detection, where subtle changes in tissue morphology or texture may indicate the presence of cancer. The proposed model can identify these patterns with high precision, aiding in early diagnosis and treatment.

Automation and Time Efficiency: The deep learning-based approach automates the process of image analysis, reducing the need for manual intervention and speeding up the diagnostic process. This is particularly valuable in clinical settings where radiologists and pathologists may be overburdened with a large volume of images to analyze. The model can process images quickly and provide accurate results, freeing up valuable time for healthcare providers to focus on patient care.

Improved Consistency and Reduced Human Error: Deep learning models do not suffer from fatigue or inconsistencies like human experts. This ensures that the model's predictions remain consistent across different cases, reducing the variability associated with human judgment. The model can also be trained on a large variety of cases, ensuring that it provides consistent results even in challenging cases.

Scalability and Adaptability: The proposed models are scalable and can be adapted for other types of cancer and medical conditions by retraining the models with new datasets. This makes them versatile tools in medical imaging, providing an opportunity for widespread adoption across different cancer types or even non-cancerous conditions.

Potential for Integration into Clinical Workflows: By integrating these deep learning models into existing clinical workflows, we can enhance the diagnostic capabilities of healthcare providers. The system can function as a decision support tool, assisting radiologists and pathologists by providing second opinions and helping identify cases that may require immediate attention.

C. COMPARISON WITH EXISTING MODEL

Table 3 represents the comparison with the existing research.

Table 3 presents a comparison of our proposed model with recent studies on the LC25000 dataset. The proposed hybrid model, combining Xception and ResNet architectures with backpropagation and SGD optimization, achieved a test accuracy of 98.96%, outperforming or matching several state-of-the-art methods in lung and colon cancer classification. For instance, it surpasses Kumar et al. who used EfficientNetB6 and obtained 93%, and Mosaad et al. who combined

TABLE 3. Comparison with existing research.

Research	Dataset Used	Methodology	Accuracy on test set
Kumar, et al., (2024) [20]	LC25000	EfficientNetB6	93%
Ochoa-Ornelas, et al., (2024) [21]	LC25000	Lightweight DNN	97.29
Kumar, Arvind, et al., (2024) [22]	LC25000	Vision Transformer	98.84%
Mosaad, Omnia Alaa, et al., (2024) [23]	LC25000	Sophisticated CNN+RNN	98.5%
Opee, et al., (2025) [24]	LC25000	lightweight model using a convolutional neural network	98.16%
Oubaalla, et al., (2024) [25]	LC25000	VGG-16	95.99%
Peng, et al., (2025) [26]	LC25000	DD-ResNet50 and ResNet50 + DE + DY	97.8% and 95.5% respectively.
Ochoa-Ornelas, et al., (2025) [27]	LC25000	MobileNetV2	97.65%
Bala, et al., (2024) [28]	LC25000	Residual Attention Networks	97.56%
Merabet, Asma, et al., (2024) [29]	LC25000	One-Shot Learning with MobileNetV2	90%
Mulyadi, et al., (2024) [30]	CRC-5000	ResNet-152 with Self-Attention	92.74%
Mulyadi, et al., (2024) [30]	CRC-5000	ResNet-50 with Self-Attention	92.13%
Our Proposed Model	LC25000	Xception and ResNet with Backpropagation and SGD	98.96%

CNN and RNN architectures achieving 98.5%. It also exceeds the performance of VGG-16 by Oubaalla et al.) at 95.99% and DD-ResNet50 by Peng et al. with 97.8%.

While the absolute gain in accuracy may appear modest, such improvements are crucial in medical diagnostics where even slight enhancements reduce the risk of misdiagnosis, ultimately benefiting patient care. Moreover, beyond accuracy, our model demonstrates practical advantages: its compact size (734.28 MB) and efficient inference time (35.06 milliseconds per image) enable real-time clinical use without sacrificing performance. This balance between accuracy, efficiency, and model complexity positions our approach as a valuable contribution to automated cancer detection systems, offering both improved diagnostic reliability and feasibility for deployment in healthcare environments.

D. IMPLICATIONS FOR CLINICAL PRACTISE AND FUTURE RESEARCH

The adoption of deep learning models for cancer diagnosis holds immense promise in transforming clinical practice and improving patient outcomes. These models can significantly enhance the speed, accuracy, and consistency of cancer detection, enabling early diagnosis and better treatment decisions.

E. CLINICAL PRACTICE

Augmentation of Clinical Decision-Making: AI-based diagnostic models can assist healthcare professionals by providing second opinions or confirming initial diagnoses. This can increase confidence in the results and help reduce diagnostic errors, especially in challenging cases where human experts might be uncertain.

Enhanced Screening Programs: The proposed models can be integrated into screening programs to detect early-stage lung and colon cancers in asymptomatic individuals. With high accuracy, the model can help identify cases that may require further investigation, leading to early interventions and improved survival rates.

Personalized Treatment Plans: AI can help healthcare providers in formulating personalized treatment plans based on the diagnosis. For example, if early-stage cancer is detected, less invasive treatments may be recommended, while advanced stages may call for more aggressive therapies. The use of AI can streamline these decision-making

processes and ensure that treatments are tailored to the specific needs of patients.

In conclusion, the proposed deep learning models for lung and colon cancer detection represent a promising step toward improving cancer diagnostics. By enhancing the speed, accuracy, and consistency of diagnoses, these models can significantly contribute to better patient outcomes. However, further research is needed to address challenges related to data quality, interpretability, and generalization to different clinical settings. As AI continues to evolve, its potential to revolutionize the field of medical diagnostics remains vast, offering numerous opportunities for improving healthcare delivery worldwide.

VI. CONCLUSION AND FUTURE WORK

In this research, we have developed a deep learning-based model using the Xception and ResNet architectures to automate the diagnosis of lung and colon cancer through histopathological images. Our primary objective was to enhance the accuracy and efficiency of cancer detection, utilizing the power of convolutional neural networks (CNNs) to identify subtle patterns in medical images that could indicate the presence of cancer. The dataset, comprising images of cancerous and non-cancerous tissues, was preprocessed through various techniques, including image augmentation and normalization, to ensure high-quality input for the model.

We integrated both Xception and ResNet models to leverage their strengths—Xception's efficiency in capturing intricate features through depthwise separable convolutions and ResNet's ability to learn deeper representations using residual connections. This architecture allowed the model to achieve high classification accuracy, outperforming traditional diagnostic methods. We employed various evaluation metrics such as accuracy, precision, recall, F1-score, and confusion matrices to measure the model's performance across different classes of lung and colon cancers.

The results demonstrated that the proposed dual-model system could significantly reduce human error, improve diagnostic consistency, and provide quicker results, all of which are critical in the clinical diagnosis of cancer. While the results of this study are promising, several avenues remain for future exploration to further enhance the system's utility and generalization:

Dataset Expansion and Diversity: The performance of the model can be improved by training on larger, more diverse datasets that encompass a broader range of imaging modalities, cancer subtypes, and patient demographics. This will help the model generalize better to new, unseen data, especially from different institutions with varying equipment and imaging techniques.

Incorporating Multimodal Data: Future work could explore the incorporation of additional data types, such as clinical data, patient histories, genetic information, and even laboratory test results, to create a more comprehensive diagnostic tool. A multimodal approach could help develop models capable of not only diagnosing cancer but also providing insights into the treatment options and prognostic outcomes.

Model Interpretability: As deep learning models are often seen as ''opaque systems,'' further research should focus on enhancing the interpretability and explainability of the predictions. It is essential to develop methods that can provide clinicians with a clearer understanding of why a specific diagnosis was made, especially in critical cases where model decisions need to be justifiable.

Real-World Validation and Deployment: One of the next most crucial steps is to validate the proposed models in real-world clinical environments. Collaborating with hospitals and medical institutions for pilot studies would provide insights into the practical challenges of deploying AI models in clinical settings and their integration into the existing workflow of healthcare professionals.

Integration with Telemedicine: AI-based diagnostic models, such as the ones developed in this research, could be integrated into telemedicine platforms for remote diagnosis and consultation, especially in underserved regions. This would not only reduce the burden on healthcare systems but also make high-quality diagnostic tools accessible to patients who might not have easy access to specialized medical care.

In conclusion, this study demonstrates the potential of deep learning models, specifically Xception and ResNet, in revolutionizing the detection and diagnosis of lung and colon cancers. By automating the analysis of histopathological images, our model improves diagnostic accuracy, reduces human error, and significantly accelerates the process of cancer detection, offering a valuable tool for clinicians in identifying early-stage cancers.

While the proposed model shows strong performance in experimental settings, the real-world application of AI in medical diagnostics presents both opportunities and challenges. Addressing the limitations related to dataset size, class imbalance, and model interpretability will be crucial for ensuring that these tools can be safely and effectively integrated into clinical workflows.

As AI continues to evolve, its role in enhancing healthcare delivery, improving patient outcomes, and streamlining medical procedures will only expand. The continued development of robust, transparent, and scalable AI-based diagnostic systems promises to bring us closer to achieving the goal of providing accurate and timely cancer diagnoses, ultimately improving the lives of patients worldwide.

REFERENCES

[1] H. Gunasekaran, S. D. Kanmani, S. Ebenezer, W. Blessing, and K. Ramalakshmi, ''Detection of lung and colon cancer using average and weighted average ensemble models,'' *EAI Endorsed Trans. Pervasive Health Technol.*, vol. 10, pp. 1–10, Feb. 2024.

[2] M. Abid, M. S. Hitam, R. Ali, H. Azami, and A. Humeau-Heurtier, ''Bidimensional increment entropy for texture analysis: Theoretical validation and application to colon cancer images,'' *Entropy*, vol. 27, no. 1, p. 80, Jan. 2025.

[3] J. Gowthamy and S. S. S. Ramesh, ''Augmented histopathology: Enhancing colon cancer detection through deep learning and ensemble techniques,'' *Microsc. Res. Technique*, vol. 88, no. 1, pp. 298–314, Jan. 2025.

[4] M. G. M. Lauande, G. Braz Junior, J. D. S. de Almeida, A. C. Silva, R. M. Gil da Costa, A. M. Teles, L. L. da Silva, H. O. Brito, F. C. B. Vidal, J. G. A. do Vale, J. R. D. Rodrigues Jr., and A. Cunha, "Building a DenseNet-based neural network with transformer and MBConv blocks for penile cancer classification," *Appl. Sci.*, vol. 14, no. 22, p. 10536, Nov. 2024.

[5] A. Muniasamy, S. A. S. Alquhtani, S. M. Bilfaqih, P. Balaji, and G. Karunakaran, "Lung cancer histopathology image classification using transfer learning with convolution neural network model," *Technol. Health Care*, vol. 32, no. 2, pp. 1199–1210, Mar. 2024.

[6] R. U. Arslan, K. A. Y. A. Ceren, and I. S. Yapici, *Deep Learning-Based Classification Framework For Colon Cancer Detection in Histopathological Images*. Commerce, CA, USA: BIDGE Publications, 2024.

[7] S. M. HaghighiKian, A. Shirinzadeh-Dastgiri, M. Vakili-Ojarood, A. Naseri, M. Barahman, A. Saberi, A. Rahmani, A. Shiri, A. Masoudi, M. Aghasipour, A. Shahbazi, Y. Ghelmani, K. Aghili, and H. Neamatzadeh, "A holistic approach to implementing artificial intelligence in lung cancer," *Indian J. Surgical Oncol.*, vol. 16, no. 1, pp. 257–278, Feb. 2025.

[8] Á. Gago-Fabero, L. Muñoz-Saavedra, J. Civit-Masot, F. Luna-Perejón, J. M. Rodríguez Corral, and M. Domínguez-Morales, "Diagnosis aid system for colorectal cancer using low computational cost deep learning architectures," *Electronics*, vol. 13, no. 12, p. 2248, Jun. 2024.

[9] A. Sharma and S. Mittal, "Lung cancer prediction using transfer learning models," in *Proc. IEEE 3rd World Conf. Appl. Intell. Comput. (AIC)*, Jul. 2024, pp. 1524–1529.

[10] F. Mercaldo, M. G. Tibaldi, L. Lombardi, L. Brunese, A. Santone, and M. Cesarelli, "An explainable method for lung cancer detection and localisation from tissue images through convolutional neural networks," *Electronics*, vol. 13, no. 7, p. 1393, Apr. 2024.

[11] A. Sobur and I. C. Rana, "Advancing cancer classification with hybrid deep learning: Image analysis for lung and colon cancer detection," *Int. J. Creative Res. Thoughts (IJCRT)*, vol. 12, no. 2, pp. c38–c45, Feb. 2024. [Online]. Available: https://www.ijcrt.org/papers/IJCRT2402237.pdf

[12] A. Seth and V. D. Kaushik, "Automatic lung and colon cancer detection using enhanced cascade convolution neural network," *Multimedia Tools Appl.*, vol. 83, no. 30, pp. 74365–74386, Feb. 2024.

[13] N. Borah, T. Agrawal, and K. S. Ali, "Effective method for cancer diagnosis employing deep learning algorithms," in *Proc. IEEE Int. Conf. Comput., Power Commun. Technol. (IC2PCT)*, Feb. 2024, pp. 995–999.

[14] M. Suominen, M. E. Subasi, and A. Subasi, "Automated detection of colon cancer from histopathological images using deep neural networks," in *Applications of Artificial Intelligence Healthcare and Biomedicine*. New York, NY, USA: Academic, 2024.

[15] M. A.-M. Provath, K. Deb, and K.-H. Jo, "Classification of lung and colon cancer using deep learning method," in *Proc. Int. Workshop Frontiers Comput. Vis.* Singapore: Springer, 2023, pp. 56–70.

[16] A. A. Khan, "Classification of colon cancer using deep learning techniques on histopathological images," *Migration Lett.*, vol. 21, no. S11, pp. 449–463, 2024.

[17] S. Tummala, S. Kadry, A. Nadeem, H. T. Rauf, and N. Gul, "An explainable classification method based on complex scaling in histopathology images for lung and colon cancer," *Diagnostics*, vol. 13, no. 9, p. 1594, Apr. 2023.

[18] O. Stephen and M. Sain, "Using deep learning with Bayesian–Gaussian inspired convolutional neural architectural search for cancer recognition and classification from histopathological image frames," *J. Healthcare Eng.*, vol. 2023, no. 1, Jan. 2023, Art. no. 4597445.

[19] R. Luo and T. Bocklitz, "A systematic study of transfer learning for colorectal cancer detection," *Informat. Med. Unlocked*, vol. 40, 2023, Art. no. 101292.

[20] V. K. D. and M. G., "Optimized deep learning approaches for lung and colon cancer classification using histopathological images," in *Proc. 3rd Int. Conf. Autom., Comput. Renew. Syst. (ICACRS)*, Dec. 2024, pp. 1665–1669.

[21] R. Ochoa-Ornelas, A. Gudiño-Ochoa, and J. A. García-Rodríguez, "A hybrid deep learning and machine learning approach with mobile-EfficientNet and grey wolf optimizer for lung and colon cancer histopathology classification," *Cancers*, vol. 16, no. 22, p. 3791, Nov. 2024.

[22] A. Kumar, R. Mehta, B. R. Reddy, and K. K. Singh, "Vision transformer based effective model for early detection and classification of lung cancer," *Social Netw. Comput. Sci.*, vol. 5, no. 7, p. 839, Aug. 2024.

[23] O. A. Mosaad, M. H. Zayyan, M. Alrahmawy, and S. Elmougy, "Lung cancer detection using hybrid convolution neural network and recurrent neural network," *Mansoura J. for Comput. Inf. Sci.*, vol. 19, no. 1, pp. 63–84, Dec. 2024.

[24] S. A. Opee, A. A. Eva, A. T. Noor, S. M. Hasan, and M. F. Mridha, "ELW-CNN: An extremely lightweight convolutional neural network for enhancing interoperability in colon and lung cancer identification using explainable AI," *Healthcare Technol. Lett.*, vol. 12, no. 1, pp. 583–595, Jan. 2025.

[25] A. Oubaalla, H. ElMoubtahij, and N. EL Akkad, "Detection of lung and colon cancer from histopathological images: Using convolutional networks and transfer learning," *Int. J. Comput. Digit. Syst.*, vol. 15, no. 1, pp. 583–595, Aug. 2024.

[26] F. Peng and S. Li, "Intelligent classification of lung cancer pathology images through comparative morphological feature learning," *Technol. Health Care*, vol. 33, no. 4, pp. 1589–1611, Jul. 2025.

[27] R. Ochoa-Ornelas, A. Gudiño-Ochoa, J. A. García-Rodríguez, and S. Uribe-Toscano, "Enhancing early lung cancer detection with MobileNet: A comprehensive transfer learning approach," *Franklin Open*, vol. 10, Mar. 2025, Art. no. 100222.

[28] D. Bala, S. M Rakib Ul Karim, and R. Ara Rasul, "MRANet: A modified residual attention networks for lung and colon cancer classification," 2024, *arXiv:2412.17700*.

[29] A. Merabet, "Innovative approaches to colon cancer imaging: Leveraging one-shot learning with MobileNetV2 feature extraction," in *Proc. Int. Conf. Artif. Intell. Appl. Age Digit. Transformation*. Cham, Switzerland: Springer, 2024, pp. 98–108.

[30] Y. F. Mulyadi and F. Utaminingrum, "Comparative analysis of ResNet architecture enhanced with self-attention for colorectal cancer detection," in *Proc. Int. Conf. Intell. Cybern. Technol. Appl. (ICICyTA)*, Dec. 2024, pp. 1089–1094.

[31] R. D. Nayagam, D. Selvathi, and H. Selvaraj, "Transfer learning approach with ResNet architecture for colon cancer classification using histopathological images," in *Models and Methods for Systems Engineering*. Cham, Switzerland: Springer, 2025, pp. 143–153.

[32] M. A. Pasha and M. Narayana, "Development of trio optimal feature extraction model for attention-based adaptive weighted RNN-based lung and colon cancer detection framework using histopathological images," *Int. J. Image Graph.*, vol. 25, no. 3, May 2025, Art. no. 2550027.

CHANDRASEKAR VENKATACHALAM received the B.E. and M.E. degrees in computer science and engineering and the Ph.D. degree in pattern recognition (biometrics) from Anna University, Chennai, in 2016. He is currently a Professor with the Computer Science and Engineering Department, Faculty of Engineering and Technology, JAIN (Deemed-to-be University), Bengaluru, India. He has 14 years of experience in the field of technical education and industry. He has published 65 papers in national and international conferences and journals. His research interests include big data analytics, software engineering, and machine learning.

PRIYANKA SHAH is currently pursuing the B.Tech. degree in computer science and engineering with JAIN (Deemed-to-be University), Bangalore, India. Her primary research interests include artificial intelligence and machine learning, with a focus on deep learning, natural language processing, and generative AI. She is dedicated to exploring AI-driven solutions for precision diagnostics and improving healthcare outcomes.